High upper critical fields of superconducting Ca10(Pt4As8)(Fe1.8Pt0.2As2)5 whiskers

Jun Li, Gufei Zhang, Wei Hu, Ya Huang, Min Ji, Han-Cong Sun, Xian-Jing Zhou, De-Yue An, Lu-Yao Hao, Qiang Zhu, Jie Yuan, Kui Jin, Hong-Xuan Guo, Daisuke Fujita, Takeshi Hatano, Kazunari Yamaura, Eiji Takayama-Muromachi, Hua-Bing Wang, Pei-Heng Wu, Johan Vanacken, and Victor V. Moshchalkov

Citation: Applied Physics Letters **106**, 262601 (2015); doi: 10.1063/1.4923216
View online: http://dx.doi.org/10.1063/1.4923216
View Table of Contents: http://scitation.aip.org/content/aip/journal/apl/106/26?ver=pdfcov
Published by the AIP Publishing

APPLIED PHYSICS LETTERS **106**, 262601 (2015)

High upper critical fields of superconducting $Ca_{10}(Pt_4As_8)(Fe_{1.8}Pt_{0.2}As_2)_5$ whiskers

Jun Li,[1,2,3,a)] Gufei Zhang,[2] Wei Hu,[4] Ya Huang,[1,3] Min Ji,[1,3] Han-Cong Sun,[1] Xian-Jing Zhou,[1,3] De-Yue An,[1,3] Lu-Yao Hao,[1] Qiang Zhu,[1] Jie Yuan,[4,3] Kui Jin,[4] Hong-Xuan Guo,[3] Daisuke Fujita,[3] Takeshi Hatano,[3] Kazunari Yamaura,[3,5] Eiji Takayama-Muromachi,[5,3] Hua-Bing Wang,[1,3,b)] Pei-Heng Wu,[1] Johan Vanacken,[2,c)] and Victor V. Moshchalkov[2]

[1]*Research Institute of Superconductor Electronics, Nanjing University, Nanjing 210093, China*
[2]*INPAC-Institute for Nanoscale Physics and Chemistry, KU Leuven, Celestijnenlaan 200D, B–3001 Leuven, Belgium*
[3]*National Institute for Materials Science, 1-2-1 Sengen, Tsukuba, Ibaraki 305-0047, Japan*
[4]*Condensed Matter Physics, Institute of Physics, Chinese Academy of Sciences, Beijing 100190, China*
[5]*Graduate School of Chemical Science and Engineering, Hokkaido University, Sapporo, Hokkaido 060-0810, Japan*

(Received 23 May 2015; accepted 16 June 2015; published online 29 June 2015)

We investigated the upper critical fields of $Ca_{10}(Pt_4As_8)(Fe_{2-x}Pt_xAs_2)_5$ superconducting whiskers. The whiskers consist of several wire-like grains with diameter of around 200 nm, joined by grain boundaries whose misorientation angles are less than 5°. The upper critical fields along *c*-axis and in *ab*-plane were observed as 49 T at 12 K and 50 T at 22 K, respectively, which can be extrapolated to ∼81 and ∼133 T at 0 K. The whisker demonstrated weak anisotropic factor and almost constant value of ∼2 below 15 K. The impressive transport properties of the whisker may find applications in fields like superconducting micro- and meso-structure systems. © *2015 AIP Publishing LLC*. [http://dx.doi.org/10.1063/1.4923216]

As a newly discovered high transition temperature (T_c) superconductor family, the Fe-based superconductors have absorbed increasingly more attentions for potential applications.[1–4] Compared with the high-T_c cuprate family, although the Fe-based superconductors have relatively lower T_c, they demonstrate nearly isotropic transport behavior, higher critical current density (J_c), similar upper critical fields (H_{c2}), and relatively higher coherence length.[1–5] Thus, the Fe-based superconductors can be applied for the high-field superconducting magnet energy storage and the energy transport as the superconducting cable or micro-devices. Until now, the highest T_c for the bulk Fe-based superconductors is 56 K for the SmFeAs(O,F) compound, whose H_{c2}^c was found as 65 T at 0 K.[6] However, the single crystals must be synthesized under an extreme condition as high pressure technique,[6] and the size of the crystals are limited to a few hundred micrometers. The best single crystal in Fe-based family comes from the AFe_2As_2 (*A* is alkali metals) system,[2–4] among which the $(Ba,K)Fe_2As_2$ exhibits the highest T_c of 38 K and H_{c2}^c of 70 T.[7,8] Another superconductor system of $Ca_{10}(Pt_4As_8)(Fe_{2-x}Pt_xAs_2)_5$ was found to have impressive T_c of 38 K, and particularly, it exhbits a layered structure with an infinite sequence of -Ca-(Pt_4As_8)-Ca-$Fe_{2-x}Pt_xAs_2$- units, where the intermediate Pt_4As_8 layer produced unusual structural and metallic characteristics.[9,10] Such metallic intermediate layers possess fundamental different transport properties from those of other multi-layer systems in both pnictide or cuprate. Mun and co-workers[11] have studied the radio-frequency contactless penetration depth measurements using pulsed magnetic fields, and estimated the H_{c2}^c of 92 T, which motivates further researches on the transport properties under high magnetic fields.

To estimate the H_{c2}, the superconductors are normally measured the magnetoresistivity or magnetization hysteresis on thin films or bulk single crystals. However, the single crystals should be fabricated into microdevices for measurements of accurate transport properties, due to the metallic behavior with low value of resistivity and high density of carriers. The Fe-based superconducting thin films have been fabricated successfully for several systems,[12–15] while not yet for the Ca-Pt-Fe-As system. Previously, we developed a method to grow superconducting $Ca_{10}(Pt_4As_8)(Fe_{1.8}Pt_{0.2}As_2)_5$ nanowhiskers directly.[16] The compounds exhibit T_c of 33 K and a single-crystalline structure with growth direction along the *a*(*b*)-axis. Since the whiskers possess micro-scaled and even nano-scaled cross-section, it is promising to evaluate the H_{c2} and J_c from the whiskers directly. In the present work, we measured the transport property of the $Ca_{10}(Pt_4As_8)(Fe_{1.8}Pt_{0.2}As_2)_5$ whiskers under pulsed high magnetic fields up to 52 T along both *ab*-plane and *c*-axis.

The relatively large-size whiskers were selected as shown in the typically topologic images characterized by a scanning helium ion microscope (SHIM, ORION Plus, Carl Zeiss) (c.f. Fig. 1). The whisker demonstrates a tile-like surface morphology, indicating the existance of grain boundaries. Each grain is observed as a width of 200–500 nm, and they are connected to each other with a misoriented angle less than 5°. For a natural growth grain boundary, the microstructures of dislocations are generally dependent on material itself. Indeed, structures of dislocations in metals and

a)junli@nju.edu.cn
b)hbwang1000@gmail.com
c)Johan.vanacken@fys.kuleuven.be

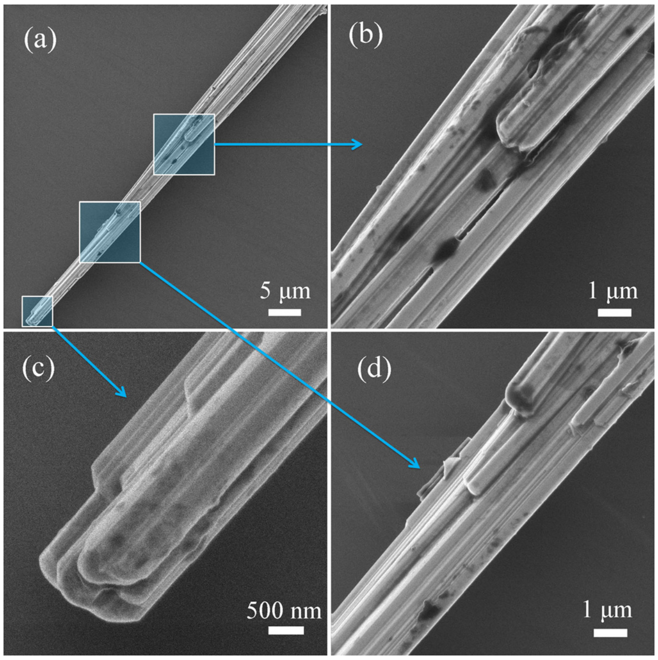

FIG. 1. Scanning helium ion microscope images of an acicular-like whisker with widths of 2–5 μm.

ceramics differ largely due to the different types of chemical bonds.[17] For the present system, we have not yet confirmed the formation mechanism of the whiskers, though we consider that the vapor-liquid-solid reaction is important,[16] which resembles the growth mechanism of Y_2BaCuO_5 nanowires studied by the *in-situ* transmission electron microscope measurements.[18]

For the transport property measurements, we fabricated a setup utilizing a photolithographic technique as shown inset of Fig. 2.[19] The contact resistance was improved as less than 0.5 Ω at room temperature. Since the resistance of whisker is relatively large enough, normally a few Ω, we can apply a low current as 100 μA. Consequently, we can inhibit the heat effects considerably. For the pulsed high magnetic fields experiments, particularly, the applied voltage should be predominant on the sample to enhance the measurement resolution. On the other hand, since the whiskers were grown along the $a(b)$-axis,[16] the resistivity along the axis of the whiskers should be the in-plane resistivity ρ_{ab}.

The temperature dependence of ρ_{ab} was measured under static magnetic fields in the Physical Properties Measurement System-9 T, Quantum Design Inc. Figure 2 shows the temperature dependence of ρ_{ab} for an individual whisker. The ρ_{ab}–T shows a linear slope within the whole temperature range, establishing a metallic-like resistivity, and the carriers are mostly from electrons. The property of $\rho_{ab}(T)$ is similar to other e-type Fe-based superconductors.[3] In contrast, the early 1048-phase crystal was found as a super-linear and even obvious low-T upturn behavior in the ρ_{ab}–T curves,[10] probably due to the crystal quality. We fit the $\rho_{ab}(T)$ in linear as shown in the figure; the results exhibit a relative high residual resistivity $\rho_0 = 72.75\,\mu\Omega$ cm. Particularly, the Pt_4As_8 intermediary layers behave as a metallic nature within the lattice structure, being different from the other structure with semiconducting Pt_3As_8 intermediary layers.[20] However, we should stress that the fitting was based on the normal state results, it is difficult to conclude the scattering profile below the T_c from the extrapolation of normal state $\rho(T)$ to low-T, unless the superconductivity can be suppressed by high magnetic fields.

The angular-dependent $\rho_{ab}(\theta)$ under $\mu_0H = 8$ T at temperatures within the superconducting transition region is shown in Fig. 3. We emphasize that the whisker was mounted onto the substrate with the wide face of the whisker, i.e., the ab-plane, parallel to the substrate, and we define the initial angle $\theta = 0$ when μ_0H is perpendicular to the substrate. Therefore, the minimum values of magnetoresistivity at 90° and 270° are accordance with situation when the μ_0H was applied within the ab-plane, while the maximum values at 0°, 180°, and 360° are corresponding to the case when μ_0H is parallel with the c-axis. On the other hand, the $\rho_{ab}(\theta)$ curves for all temperatures demonstrate continuous fluctuation with absence of abrupt steps, indicating that the grains within the

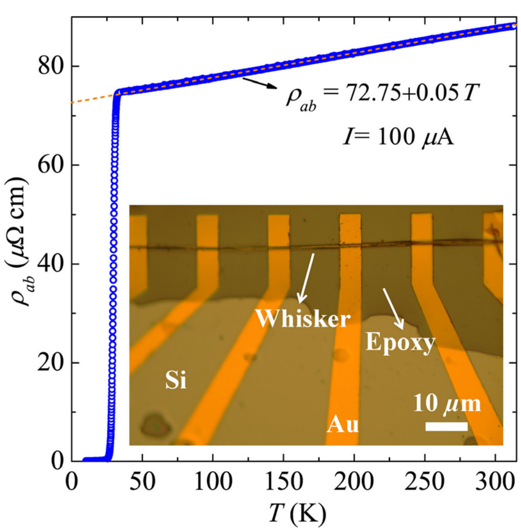

FIG. 2. Temperature dependence of resistivity ρ_{ab} without field. Here, we used the ac-measurement method with frequency of 997 Hz. The orange dash line indicates T-linear fitting for ρ_{ab} as $\rho_{ab} = \rho_0 + kT$. The inset shows an optical image for the resistivity measurement device from an individual whisker with width of ~2 μm and thickness of ~0.5 μm.

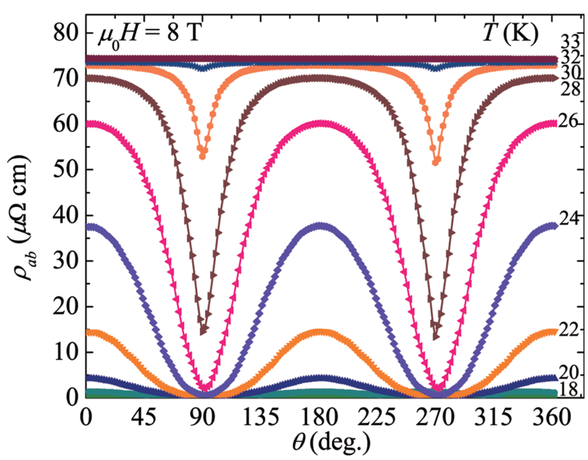

FIG. 3. Angular-dependence magnetoresistivity $\rho_{ab}(\theta)$ for the whisker under magnetic field of 8 T, where θ means the angle between μ_0H and c-axis. Here, we used the ac-measurement method with frequency of 997 Hz. The maximum resistance was observed at angles of 0°, 180°, and 360°, where μ_0H is parallel with c-axis.

whisker are well-orientated; namely, the c-axes of the grains are parallel with each other as can be seen from Fig. 1.

Based on the calibrated c-axis orientation from the $\rho_{ab}(\theta)$ results in Fig. 3, confirmed lattice orientation, the isothermal magnetoresistivity of the whisker was also characterized under pulsed high magnetic fields up to 52 T in KU Leuven,[21] as shown in Figs. 4(a) and 4(b). Since there is no hysteresis for ρ_{ab} under $\mu_0 H$ sweep up and down processes, we selected the data during the sweep up process. For the $\mu_0 H$ applied along the c-axis, the $\rho_{ab}(H)$ exhibits a sharp transition at relatively high temperature region, while a broadened transition is observed as cooling down. As the $\mu_0 H$ perpendicular with the c-axis, superconductivity is strongly against the $\mu_0 H$, indicating anisotropic properties. Note that the $\mu_0 H$ up to 52 T can suppress the superconductivity at temperatures down to 8 and 22 K for the field along the c-axis and within the ab-plane, respectively. On the other hand, since the values of normal state resistance are almost temperature-independent, we assume that they are the same value of the normal state resistance at the transition temperature, $R_n(T_c)$. The horizontal dash dot lines indicate 10%, 50%, and 90% of the resistive transition relative to $R_n(T_c)$, respectively.

Figures 4(c) and 4(d) show the temperature-dependent resistivity under zero and pulsed high fields for the fields applied along the c-axis and within the ab-plane. For $\mu_0 H$ from 5 to 45 T, the $\rho_{ab}(T)$ curves demonstrate monotonical increases with temperature regardless of $H \perp c$-axis or $H // c$-axis. Particularly, the $\rho_{ab}(T)$ curves below the T_c are still accordance with the linear relation from the high-temperature region shown in Fig. 2. Previously, a low-T

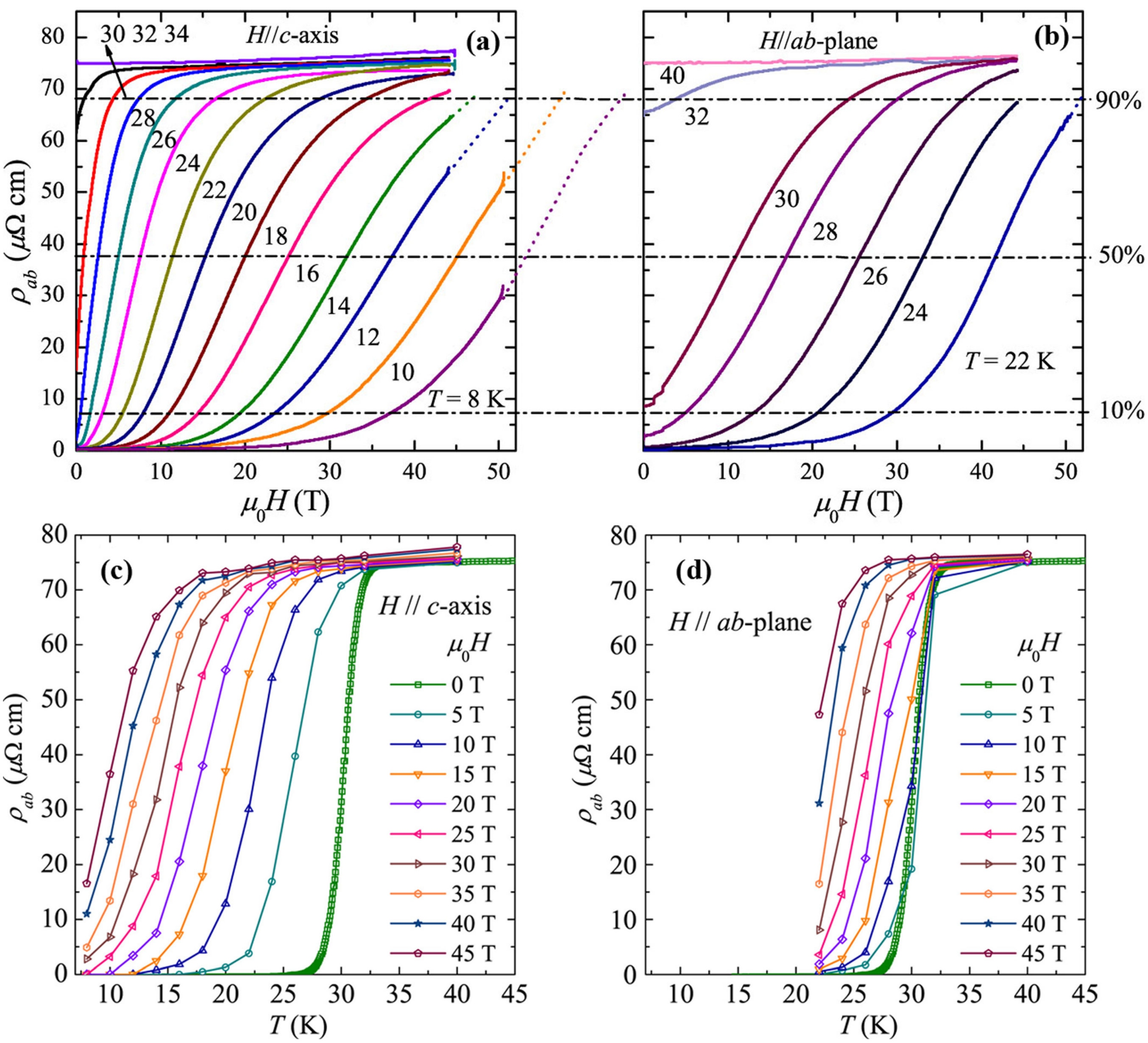

FIG. 4. Pulsed magnetic fields dependence of resistivity at various temperatures for the whisker. Here, we used the ac-measurement method with frequency of 7.77 kHz. The fields were applied along different directions of (a) the c-axis and (b) the ab-plane. The dot lines in (a) demonstrate to the extrapolated ρ–H curves. The values of H_{c2} are determined by the cross-over points of the ρ–H curves and the corresponding resistivity lines. The bias currents were 100 μA for all measurements. Temperature dependent of resistivity under zero and pulsed high fields for the fields applied (c) along the c-axis and (d) within the ab-plane. The bias currents were 100 μA for all measurements.

upturn or metal-insulator-like phenomenon was generally observed for the superconductivity suppressed by high magnetic fields,[22,23] which corresponded to charge carrier localization, under-doped case, or even crystal quality with a second phase. Therefore, the $\rho_{ab}(T)$ curves of present results reveal the high quality of the whisker and optimally doped case as well. In addition, the linear $\rho_{ab}(T)$ behavior below the T_c can also indicate that the charge carriers retain electron type. For the $H//c$-axis, the $\rho_{ab}(T)$ curves show almost parallel shift with increase of magnetic fields, and the superconductivity can exist at temperature below 15 K under $\mu_0 H = 45$ T. However, the superconductivity can be against $\mu_0 H = 45$ T at temperatures up to 25 K for $H//ab$-plane.

Based on the results from Fig. 4, we estimated the temperature dependent upper critical fields along the c-axis H_{c2}^{c} and in the ab-plane H_{c2}^{ab} shown in Fig. 5. The H_{c2}^{ab} is observed as considerably larger than the H_{c2}^{c}, and demonstrates different temperature dependent profiles. Since the gap-symmetry of Fe-based superconductors was generally considered as a two-band model in combination with orbital-limiting,[24–27] we employ a two-band s-wave model to fit the present experimental data. The fitting results are given in Fig. 5. We took the same coupling constants for the intra- and inter-coupling $\lambda_{12} = \lambda_{21} = 0.5$, $\lambda_{11} = 0.5$, and $\lambda_{12} = 1.01$ for different definitions and field orientations. As discussed by Hunte[24] and Kano,[25] the results here are not sensitive to the choice of the coupling constants. Thus, we can extrapolate the H_{c2}^{ab} and H_{c2}^{c} to 0 K, and estimate the $H_{c2}^{ab}(0\,\text{K})$ and H_{c2}^{c} (0 K) to 133.61 and 81.37 T, respectively.

The upper critical field anisotropic factor is estimated from $\gamma_H = H_{c2}^{ab}(T)/H_{c2}^{c}(T)$. The γ_H reveals a value of ∼10 at temperatures nearby the T_c, and gradually decreases with temperatures until an almost constant value (∼2) below 15 K. The results exhibit that the anisotropy of $Ca_{10}(Pt_4As_8)(Fe_{1.8}Pt_{0.2}As_2)_5$ is similar to those of the double-layered and the single-layered Fe-based superconductors, for instance, the 122-type and 11-type.[17] However, recent study found that the multi-layered 12311-type $(V_2Sr_4O_6)Fe_2As_2$ superconductor ($\gamma_H = 51$) shows considerably larger anisotropy than the 1048-type superconductors, although both superconductors are characterized as multi-layer.[28] The 12311-type crystal was observed intrinsic Josephson effects along the c-axis revealing a semiconductor behavior, while the c-axis transport of the 1048-type is still metallic. Moreover, the 1111-type crystals exhibit stronger anisotropic properties than the present crystal as well, which could be attributed to an insulating layer AO (A is La, Sm, Dy,…) between the superconducting layers Fe_2As_2.[17]

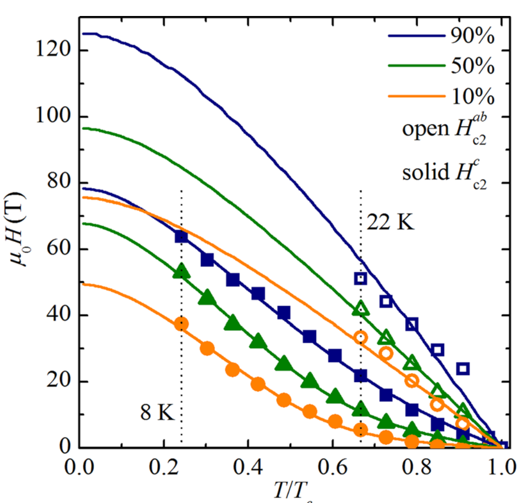

FIG. 5. $H_{c2}(T)$ obtained from 10%, 50%, and 90% transition are plotted as function of the normalized temperature T/T_c. The solid lines correspond to $H_{c2}(T)$ calculated from two-band theory.

In summary, $Ca_{10}(Pt_4As_8)(Fe_{1.8}Pt_{0.2}As_2)_5$ whiskers were studied by measuring their magnetoresistivity under pulsed high magnetic fields. The upper critical fields were found to be 49 T at 12 K along c-axis and 50 T at 22 K in the ab-plane, extrapolating to upper critical fields at 0 K of 81.37 T along c-axis and 133.61 T in the ab-plane. The whisker demonstrated weak anisotropic factor and almost constant value of ∼2 below 15 K. The temperature dependent upper critical fields can be well explained by the multi-gap s-wave model, being consistent with the other iron-based superconductors.

This research was supported by the National Natural Science Foundation of China (Nos. 11234006 and 51102188), the Priority Academic Program Development of Jiangsu Higher Education Institutions, Methusalem Funding by the Flemish Government, the EU-FP6-COST Action MP1201, the Priority Academic Program Development of Jiangsu Higher Education Institutions, the "Strategic Priority Research Program" of the Chinese Academy of Sciences (No. XDB07010100), the World Premier International Research Center from MEXT, the Grants-in-Aid for Scientific Research (Nos. 25289108, 25289233, and 25289108) from JSPS, and the Funding Program for World-Leading Innovative R&D on Science and Technology (FIRST Program) from JSPS.

[1]Y. Kamihara, T. Watanabe, M. Hirano, and H. Hosono, J. Am. Chem. Soc. **130**, 3296 (2008).
[2]J. Paglione and R. L. Greene, Nat. Phys. **6**, 645 (2010).
[3]P. D. Johnson, G. Xu, and W. G. Yin, *Iron-based Superconductivity* (Springer, 2015).
[4]I. I. Mazin, Nature **464**, 183 (2010).
[5]P. Seidel, Supercond. Sci. Technol. **24**, 043001 (2011).
[6]P. J. W. Moll, R. Puzniak, F. Balakirev, K. Rogacki, J. Karpinski, N. D. Zhigadlo, and B. Batlogg, Nat. Mater. **9**, 628–633 (2010).
[7]H. Q. Yuan, J. Singleton, F. F. Balakirev, S. A. Baily, G. F. Chen, J. L. Luo, and N. L. Wang, Nature **457**, 565 (2009).
[8]M. M. Altarawneh, K. Collar, C. H. Mielke, N. Ni, S. L. Bud'ko, and P. C. Canfield, Phys. Rev. B **78**, 220505(R) (2008).
[9]S. Kakiya, K. Kudo, Y. Nishikubo, K. Oku, E. Nishibori, H. Sawa, T. Amamoto, T. Nozaka, and M. Nohara, J. Phys. Soc. Jpn. **80**, 093704 (2011).
[10]N. Ni, J. M. Allred, B. C. Chan, and R. J. Cava, Proc. Natl. Acad. Sci. U. S. A. **108**, E1019 (2011).
[11]E. Mun, N. Ni, J. M. Allred, R. J. Cava, O. Ayala, R. D. McDonald, N. Harrison, and V. S. Zapf, Phys. Rev. B **85**, 100502(R) (2012).
[12]K. Iida, J. Hänisch, E. Reich, F. Kurth, R. Hühne, L. Schultz, B. Holzapfel, A. Ichinose, M. Hanawa, I. Tsukada, M. Schulze, S. Aswartham, S. Wurmehl, and B. Büchner, Phys. Rev. B **87**, 104510 (2013).
[13]S. Lee, J. Jiang, Y. Zhang, C. W. Bark, J. D. Weiss, C. Tarantini, C. T. Nelson, H. W. Jang, C. M. Folkman, S. H. Baek, A. Polyanskii, D. Abraimov, A. Yamamoto, J. W. Park, X. Q. Pan, E. E. Hellstrom, D. C. Larbalestier, and C. B. Eom, Nat. Mater. **9**, 397 (2010).
[14]T. Katase, Y. Ishimaru, A. Tsukamoto, H. Hiramatsu, T. Kamiya, K. Tanabe, and H. Hosono, Nat. Commun. **2**, 409 (2011).
[15]M. Kidszun, S. Haindl, T. Thersleff, J. Hänisch, A. Kauffmann, K. Iida, J. Freudenberger, L. Schultz, and B. Holzapfel, Phys. Rev. Lett. **106**, 137001 (2011).

[16]J. Li, J. Yuan, D.-M. Tang, S.-B. Zhang, M.-Y. Li, Y. F. Guo, Y. Tsujimoto, T. Hatano, S. Arisawa, D. Golberg, H.-B. Wang, K. Yamaura, and E. Takayama-Muromachi, J. Am. Chem. Soc. **134**, 4068 (2012).
[17]H. Hilgenkamp and J. Mannhart, Rev. Mod. Phys. **74**, 485 (2002).
[18]R. Boston, Z. Schnepp, Y. Nemoto, Y. Sakka, and S. R. Hall, Science **344**, 623 (2014).
[19]J. Li, J. Yuan, M. Ji, G. Zhang, J.-Y. Ge, H.-L. Feng, Y.-H. Yuan, T. Hatano, W. Hu, K. Jin, T. Schwarz, R. Kleiner, D. Koelle, K. Yamaura, H.-B. Wang, P.-H. Wu, E. Takayama-Muromachi, J. Vanacken, and V. V. Moshchalkov, Phys. Rev. B **90**, 024512 (2014).
[20]M. Neupane, C. Liu, S.-Y. Xu, Y.-J. Wang, N. Ni, J. M. Allred, L. A. Wray, N. Alidoust, H. Lin, R. S. Markiewicz, A. Bansil, R. J. Cava, and M. Z. Hasan, Phys. Rev. B **85**, 094510 (2012).
[21]J. Vanacken, T. Peng, J. A. A. J. Perenboom, F. Herlach, and V. V. Moshchalkov, J. Low Temp. Phys. **170**, 553–561 (2013).
[22]D. LeBoeuf, N. Doiron-Leyraud, J. Levallois, R. Daou, J.-B. Bonnemaison, N. E. Hussey, L. Balicas, B. J. Ramshaw, R. Liang, D. A. Bonn, W. N. Hardy, S. Adachi, C. Proust, and L. Taillefer, Nature **450**, 533 (2007).
[23]D. LeBoeuf, N. Doiron-Leyraud, B. Vignolle, M. Sutherland, B. J. Ramshaw, J. Levallois, R. Daou, F. Laliberte, O. Cyr-Choiniere, J. Chang, Y. J. Jo, L. Balicas, R. Liang, D. A. Bonn, W. N. Hardy, C. Proust, and L. Taillefer, Phys. Rev. B **83**, 054506 (2011).
[24]F. Hunte, J. Jaroszynski, A. Gurevich, D. C. Larbalestier, R. Jin, A. S. Sefat, M. A. McGuire, B. C. Sales, D. K. Christen, and D. Mandrus, Nature **453**, 903 (2008).
[25]M. Kano, Y. Kohama, D. Graf, F. Balakirev, A. S. Sefat, M. A. Mcguire, B. C. Sales, D. Mandrus, and S. W. Tozer, J. Phys. Soc. Jpn. **78**, 084719 (2009).
[26]A. Gurevich, Phys. Rev. B **67**, 184515 (2003).
[27]G. Wu, R. L. Greene, A. P. Reyes, P. L. Kuhns, W. G. Moulton, B. Wu, F. Wu, and W. G. Clark, J. Phys.: Condens. Matter **26**, 405701 (2014).
[28]P. J. W. Moll, X. Zhu, P. Cheng, H.-H. Wen, and B. Batlogg, Nat. Phys. **10**, 644–647 (2014).